

Yielding behavior and its effect on uniform elongation in IF steel with various grain sizes

Si Gao · Meichuan Chen · Mohit Joshi ·
Akinobu Shibata · Nobuhiro Tsuji

Received: 2 March 2014 / Accepted: 7 April 2014 / Published online: 24 April 2014
© Springer Science+Business Media New York 2014

Abstract In the present study, IF steel specimens with different grain sizes ranging from 12 to 0.45 μm were fabricated by accumulative roll-bonding process and subsequent annealing. Tensile tests revealed that by decreasing the mean grain size down to an ultrafine range smaller than approximately 1.5 μm , yielding behavior of the IF steel gradually changed from continuous yielding to discontinuous yielding. An abrupt loss in the uniform elongation occurred, when the average grain size was smaller than about 1 μm . Hall–Petch analysis on the yield stress and uniform elongation implied that the abrupt loss in the uniform elongation in the UFG grain size range corresponded to the appearance of the discontinuous yielding behavior. As it has been found in many UFG materials, discontinuous yielding is believed to be a unique mechanical behavior of UFG materials, and it has significant importance on the uniform elongation of UFG materials.

Introduction

According to the well-known Hall–Petch relation, yield stress of polycrystalline materials increases with decreasing the average grain size [1], [2]:

$$\sigma_y = \sigma_0 + k_y d^{-1/2}. \quad (1)$$

S. Gao (✉) · M. Chen · M. Joshi · A. Shibata · N. Tsuji
Department of Materials Science and Engineering, Kyoto
University, Kyoto, Japan
e-mail: si.gao@tsujilab.mtl.kyoto-u.ac.jp

A. Shibata · N. Tsuji
Elements Strategy Initiative for Structural Materials (ESISM),
Kyoto University, Kyoto, Japan

where σ_y is yield stress, σ_0 friction stress, k_y a constant (Hall–Petch slope), and d the mean grain size. Significant grain size refinement could be recently achieved by severe plastic deformation (SPD) processes, which has led to a very high strength according to the Hall–Petch relation, but has also led to limited ductility [3]. Other unique mechanical properties have been found in those nanostructured metals fabricated by SPD processes. Huang et al. [4], [5] found that in accumulative roll-bonding (ARB) processed Al and interstitial free (IF) steel, the strength decreased by deformation, while it increased by annealing. This interesting behavior, so called “hardening by annealing and softening by deformation”, is totally opposite from the commonsense in conventional metals which usually exhibit hardening by deformation and softening by annealing. The elongation of the material was also found to be closely related to the hardening and softening phenomena: the nanostructured material hardened by annealing exhibit a reduction in elongation, while the material softened by deformation shows an increased elongation. Huang et al. systematically investigated the effect of subsequent cold deformation and annealing on the elongation of the ARB processed Al alloys and IF steel [4], [5], [6], and concluded that the dislocation density is the critical parameter for this unique behavior: the deformation becomes more homogeneous by introducing dislocations, while more inhomogeneous by decreasing the free dislocations.

On the other hand, the yield point phenomenon (or discontinuous yielding) has been found in many nanostructured metals such as Cu [7], Al [3], [8], and Ti [9], although it is well known that those materials exhibit continuous yielding behavior with in the coarse-grained state. Yield point phenomenon was firstly found in low-carbon steels, which is characterized by a distinct yield

drop and subsequent Lüders-band type deformation. It is generally believed that the yield point phenomenon in the materials is attributed to the lack of initial mobile dislocations [8].

The “hardening by annealing and softening by deformation” in nanostructured metals might be explained from the viewpoint of yielding behavior. In the present study, the IF steel specimens with different grain sizes were fabricated by the ARB process and subsequently annealing. In the present paper, we firstly demonstrate that the dramatic loss in the uniform elongation of the fine grain specimens is attributed to the appearance of yield point phenomenon using the Hall–Petch analysis for the yield and flow stresses. Then, it is shown that enhancement and reduction in the uniform elongation could be achieved by altering the yielding behavior of the fine-grained IF steel specimen.

Experimental procedure

The chemical composition of the IF steel used in this study is given in Table 1. The starting material has a fully recrystallized microstructure with an average grain size of around 30 μm . The starting sheet having 2 mm thickness, 5 mm width, and 30 mm length was rolled at 500 $^{\circ}\text{C}$ by 50 % reduction in one pass without lubrication. Then, the sheet having 1 mm thickness was cut, stacked, and roll-bonded at 500 $^{\circ}\text{C}$ by a 50 % reduction without lubrication again. Up to five cycles of the ARB process were repeatedly carried out on the specimen after the first 50 % rolling. After the first 50 % rolling and subsequent five cycles of the ARB process, the total reduction in thickness of 98.4 % or equivalent strain of 4.8 was imposed to the sheet. The ARB processed specimens were annealed in a salt bath at different temperatures ranging from 500 $^{\circ}\text{C}$ to 800 $^{\circ}\text{C}$ for 30 min in order to obtain different average grain sizes, then quenched into water. Microstructures of the deformed and annealed specimens were observed by electron back-scattering diffraction (EBSD) analysis in a field emission-type scanning electron microscope (FE-SEM). The observations were carried out on longitudinal sections perpendicular to the transverse direction (TD) of the sheets. Average grain sizes of the specimens were determined by the linear interception method using EBSD grain boundary maps. Mechanical properties were evaluated by tensile test at ambient temperature with an initial strain rate of $8.3 \times 10^{-4} \text{ s}^{-1}$. Tensile test specimens with 10 mm in gauge length and 5 mm in gauge width were cut from the ARB processed and annealed sheets, so as to make the tensile axis parallel to RD. During tensile test, an extensometer was attached on the specimen to precisely measure the displacement. A digital CCD camera was used in some

Table 1 Chemical composition of the IF steel used in this study (mass %)

C	N	Si	Mn	P	S	Al	Ti	Fe
0.002	0.0027	0.01	0.10	0.005	0.006	0.032	0.039	Bal.

of the tensile tests in order to capture the surface morphology of the specimens during tensile deformation.

Results

EBSD grain boundary maps of four specimens are selected to demonstrate the typical microstructures of deformed and annealed specimen, as shown in Fig. 1. In the figure, very small angle boundaries with misorientation smaller than 2° , low angle boundaries with misorientation between 2° and 15° , and high angle boundaries with misorientation larger than 15° are drawn in red, green, and blue lines, respectively. The as-ARB processed specimen has elongated ultrafine grains surrounded mostly by high angle grain boundaries, with a mean grain size (thickness) of 0.3 μm (Fig. 1a), which is a typical microstructure after the ARB process [10]. After annealing at 500 $^{\circ}\text{C}$ for 30 min, coarsening of the microstructure is recognized in Fig. 1b. With further increasing the annealing temperature to 560 $^{\circ}\text{C}$, the majority of the structures shows an almost equiaxed morphology as shown in Fig. 1c. A complete equiaxed microstructure was obtained in the specimen annealed at higher temperatures, for example, at 600 $^{\circ}\text{C}$, as shown in Fig. 1d. The average grain size of the four specimens shown in Fig. 1 is 0.45, 0.65, 0.85, or 2.8 μm , respectively. Larger grain sizes with equiaxed morphology were obtained by higher annealing temperatures above 600 $^{\circ}\text{C}$.

Nominal stress–strain curves of the as-ARB and annealed specimens are shown in Fig. 2. Their average grain sizes are indicated in the figure. The as-ARB processed specimen with the mean grain size of 0.45 μm shows very high yield strength (720 MPa) and quite limited uniform and total elongation (1.3 and 4.2 %). With increasing the mean grain size by rising the annealing temperature, the strength decreases and elongation increases, as generally observed in the ARB processed and subsequently annealed materials [10]. It is noteworthy that the specimens with ultrafine grain sizes ($d = 0.45\text{--}0.95 \mu\text{m}$) exhibit discontinuous yielding characterized by a clear yield point phenomenon, while the larger grain-sized specimens ($d > 1.5 \mu\text{m}$) exhibit continuous yielding. Macroscopically homogeneous deformation occurs in those coarse grain-sized specimens exhibiting continuous yielding, as shown in Fig. 3a. When the discontinuous yielding

Fig. 1 EBSD boundary maps of the IF steel specimens ARB processed to an equivalent strain of 4.8 and subsequently annealed at various temperatures for 1.8 ks. **a** As ARB processed. **b** Annealed at 500 °C. **c** Annealed at 560 °C. **d** Annealed at 600 °C

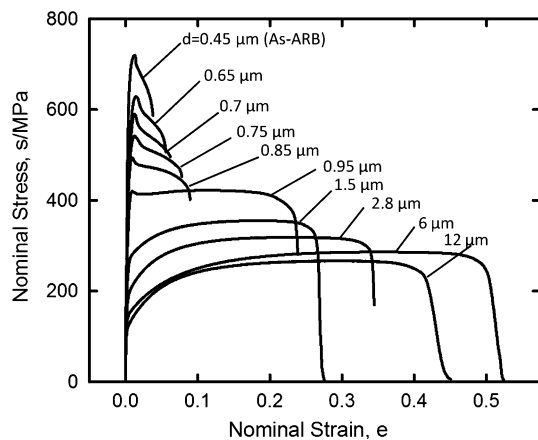
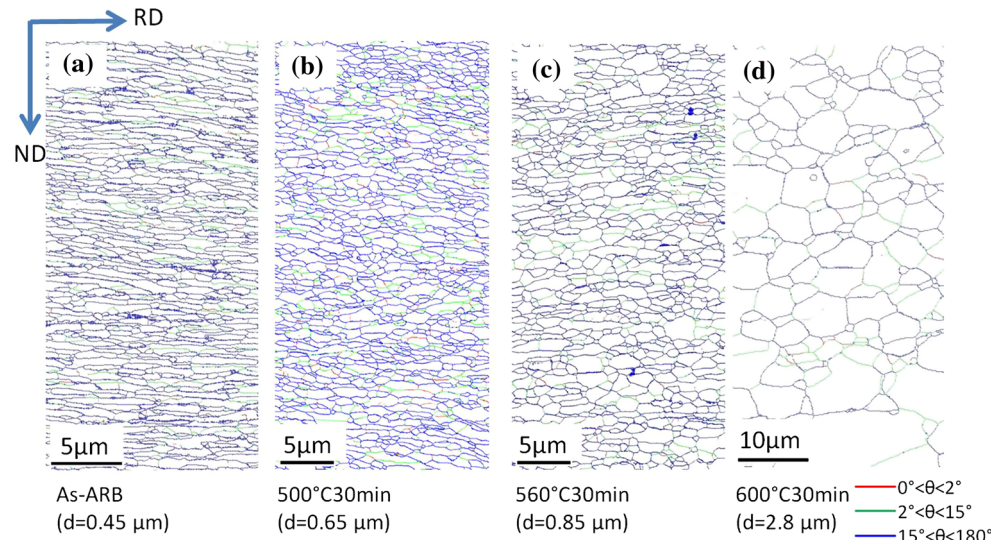


Fig. 2 Nominal stress–strain curves of the ARB processed and annealed IF steel with various mean grain sizes ranging from 12 to 0.45 μm

occurred in the specimens with fine grain sizes, Lüders deformation was observed. An example in the specimen having $d = 0.95 \mu\text{m}$ is shown in Fig. 3b. In the specimens whose grain sizes are smaller than $0.95 \mu\text{m}$, macroscopic necking immediately occurred after the yield point and localized shear bands were observed on the surface of the tensile specimens, as shown in Fig. 3c.

Yield stress obtained from the tensile test is plotted as a function of $d^{-1/2}$ in Fig. 4 (Hall–Petch plot). The upper yield stress (yield point stress) was taken as the yield stress for the specimens exhibiting clear yield point phenomenon, while the 0.2 % offset proof stress was taken as the yield stress for the specimens exhibiting continuous yielding. It is seen that two distinct Hall–Petch relations are obtained depending on the average grain size range, with the different values of k_y and σ_0 given in the figure. In the larger grain size range ($d = 1.5\text{--}12 \mu\text{m}$), a low k_y value is

obtained by linear fitting, which is comparable with previous results from conventionally coarse-grained specimens [11]. While in the fine grain size range ($d = 0.65\text{--}0.95 \mu\text{m}$), a very high k_y value and a negative σ_0 is obtained. It has been clarified in the parallel studies by the present authors that the high k_y value is associated with the discontinuous yielding behavior in the fine grain size range [11]. The yield stress of the as-ARB processed specimen, however, deviates from the extrapolated Hall–Petch relation having larger k in Fig. 4, which should be attributed to the deformed microstructures after ARB process [10].

The uniform elongation values of the IF steel specimens are plotted as a function of $d^{-1/2}$ in Fig. 5. It is seen that the uniform elongation slightly increases, and then continuously decreases with decreasing the mean grain size (d) from 12 to $1.5 \mu\text{m}$. A dramatic drop in the uniform elongation is observed as the grain size becomes smaller than $1.5 \mu\text{m}$. When the grain size is smaller than $0.95 \mu\text{m}$, the uniform elongation becomes very low, smaller than 1.5 %.

Discussion

Yield point phenomenon

Yield point phenomenon often occurs in the materials having a strong dislocation–impurity interaction, such as iron with interstitial carbon and nitrogen. According to Cottrell and Bilby theory in 1950s [12], the yield point is attributed to the dislocation locking by impurity atoms. Stress drop corresponds to making dislocations free from the atmosphere of impurity atoms. Later, Hahn [13] proposed the mobile dislocation density model by considering

Fig. 3 Surface appearances of the tensile specimens with various mean grain sizes. **a** $d = 12 \mu\text{m}$ at tensile strain $\epsilon = 0.25$, **b** $d = 0.95 \mu\text{m}$ at $\epsilon = 0.1$, and **c** $d = 0.75 \mu\text{m}$ at $\epsilon = 0.03$

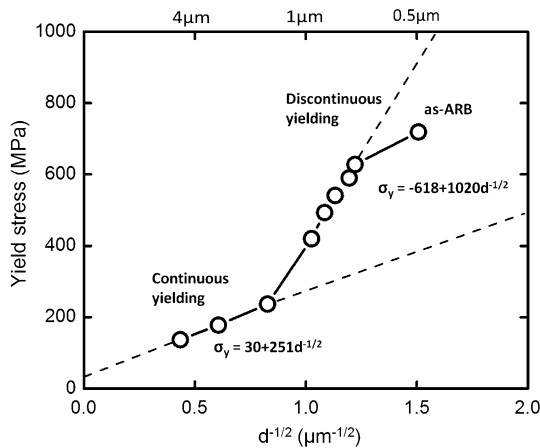
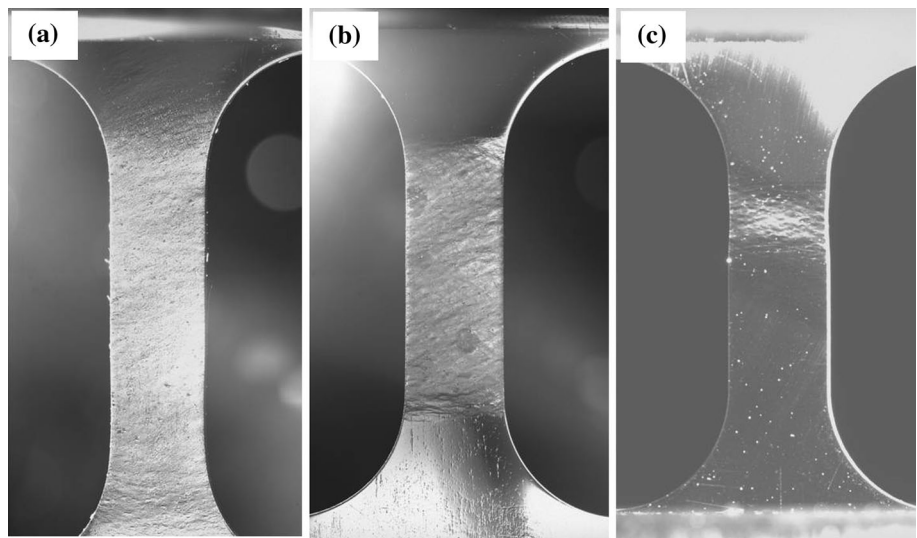


Fig. 4 Yield stress of the IF steel specimens plotted as a function of inverse square root of the mean grain size (Hall–Petch plot). The Hall–Petch relations obtained from the specimens which show continuous or discontinuous yielding behaviors are also represented in different broken lines

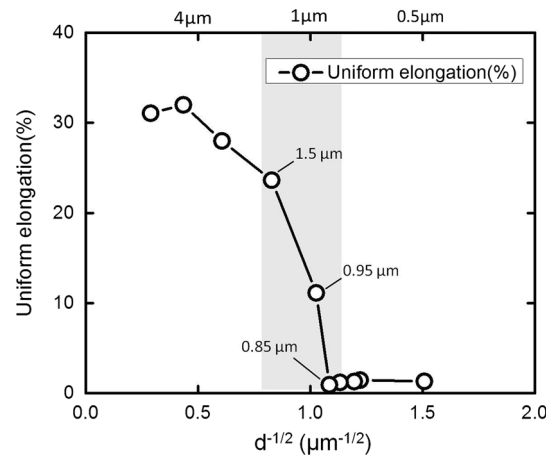


Fig. 5 Uniform elongation of the IF steel specimens plotted as a function of inverse square root of the mean grain size. A dramatic drop in the uniform elongation occurs in the *gray* colored range ($0.85 \mu\text{m} < d < 1.5 \mu\text{m}$)

the relationship between of dislocation velocity and mobile dislocation density, and attributed yield point phenomenon to the lack of initial mobile dislocation density and sudden multiplication of mobile dislocations. It is obvious that the dislocation locking mechanism cannot explain the yield point phenomenon in the present study because interstitial carbon and nitrogen atoms are fixed by titanium to form carbide and nitride in the present IF steel. In recent years, the yield point phenomenon has been more and more found to occur in fine-grained materials such as pure Cu [7], Al [3], Ti and their alloys [9], [7], [14], and austenitic steels [15], all of which do not exhibit yield point in the coarse-grained microstructures. It is likely that Hahn’s model is applied to explain the yield point phenomenon in the fine-grained materials. Since the mobile dislocation density

required to initiate plastic deformation increases with decreasing the average grain size, it is generally believed that the initial mobile dislocation density (or dislocation source density) is inherently insufficient in these fine grain-sized materials with limited volumes (especially after annealing) [8]. As a result, the yield point phenomenon occurs in such fine-grained materials. However, systematic investigation is still necessary to clarify this interesting phenomenon quantitatively.

Dramatic drop in uniform elongation

It is noteworthy that the uniform elongation dramatically drops to less than 1.5 % as the average grain size decreases down to values smaller than $0.95 \mu\text{m}$ in Fig. 5. This sudden

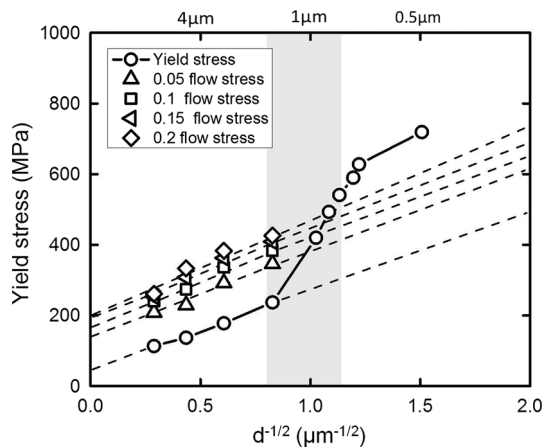


Fig. 6 Flow stresses at 0.05, 0.1, 0.15, and 0.2 true strains plotted against the inverse square root of the mean grain size. The Hall–Petch slopes for the flow stresses at given strains show similar values of around $250 \text{ MPa } \mu\text{m}^{1/2}$. The gray area indicates the grain size range where yield point phenomenon occurs and the sudden drop in uniform elongation occurs

drop in uniform elongation can be also explained by the Hall–Petch analysis for the yield stress and flow stresses. In Fig. 6, the yield stress and flow stresses at true strains of 0.05, 0.1, 0.15, 0.2, which are obtained from true stress–strain curves of the coarse-grain-sized specimens, are plotted as a function of $d^{-1/2}$. For the fine grain size specimens, the uniform elongation is too small to measure the flow stress from the true stress strain curves. It is known that the Hall–Petch relation can be applied not only for the yield stress but also for the flow stress at a given strain [16]:

$$\sigma_{\varepsilon} = \sigma_{0\varepsilon} + k\varepsilon d^{-1/2} \quad (2)$$

where σ_{ε} , $\sigma_{0\varepsilon}$ and k_{ε} are the flow stress, friction stress and Hall–Petch slope at a given strain, respectively. It is found in Fig. 6 that the flow stresses at given true strains also follow Hall–Petch relation with a slope similar to that for the yield stress in the coarse grain size range. However, because of the higher Hall–Petch slope for the yield stress in the fine grain size range, the yield stress increases more rapidly than the flow stress with decreasing the grain size. When the mean grain size becomes smaller than $0.95 \mu\text{m}$, the yield stress eventually intersects with and soon exceeds the flow stresses in the Hall–Petch plot in Fig. 6. When the yield stress exceeds the extrapolated flow stress, a strain localization occurs at the onset of yielding, namely yield point phenomenon (or discontinuous yielding) in the present study. At medium grain sizes, for example $0.95 \mu\text{m}$, the yield stress is between the flow stress at 0.05 and 0.1 strain, which indicates that the strain localization in this specimen is not significant. This can be confirmed by the stress–strain

curve of this specimen, which still shows a uniform strain hardening part after the yield point and Lüders deformation. As the grain size becomes smaller than $0.85 \mu\text{m}$, the yield stress already reaches or even exceeds the flow stress at 0.2 strain, indicating significant strain localization should happen at the onset of yielding. This leads to the macroscopic necking immediately after yielding, as shown by the highly localized shear bands on the specimen shown in Fig. 3, and by the stress–strain curves shown in Fig. 2. It should be noted that overtaking of the yield stress over the flow stresses occurs in a very narrow grain size range (from $d = 1.5$ to $0.85 \mu\text{m}$, indicated in gray range in Fig. 6) which coincides with the same grain size range (indicated in gray range in Fig. 5) where the uniform elongation suddenly drops to less than 2 %. This means that the abrupt drop in the uniform elongation in the fine grain size range results from the appearance of the discontinuous yielding behavior.

Effect of yielding behavior on uniform elongation

Since the abrupt loss in uniform elongation is due to the discontinuous yielding behavior in the fine grain size range, it is expected to improve the uniform elongation by modifying the yielding behavior of the material. Temper rolling is usually applied in sheet steel industries to diminish the Lüders deformation by introducing mobile dislocations in the materials [17]. In the present study, the same principle is used, that is, introducing mobile dislocations to the material by temper rolling to change the discontinuous yielding into continuous yielding behavior. Specimens with a nearly equiaxed microstructure ($d = 0.85 \mu\text{m}$) were prepared by the ARB process with a total strain of 4.8 and subsequent annealing at $560 \text{ }^{\circ}\text{C}$ for 30 min. The stress–strain curve of the specimen is shown as curve 1 in Fig. 7. The ARB processed and $560 \text{ }^{\circ}\text{C}$ annealed specimen exhibits a clear yield point phenomenon and very low uniform elongation of 0.94 %. One of such specimens was subjected to a temper rolling of 5 % reduction at room temperature and then tensile tested. It is found that the yield point phenomenon is removed by the temper rolling in curve 2 in Fig. 7. The stress–strain curve (curve 2) exhibits a more continuous yielding behavior compared with curve 1, with a slight decrease in the ultimate tensile strength (from 482 to 475 MPa), but a significant increase in the uniform elongation (from 0.94 to 6.7 %). In order to furthermore demonstrate the effect of yielding behavior on the uniform elongation, a low temperature annealing at $450 \text{ }^{\circ}\text{C}$ for 120 min was carried out on the specimen ARB processed, $560 \text{ }^{\circ}\text{C}$ annealed and 5 % temper rolled for decreasing the mobile dislocation density without significant change in the grain size

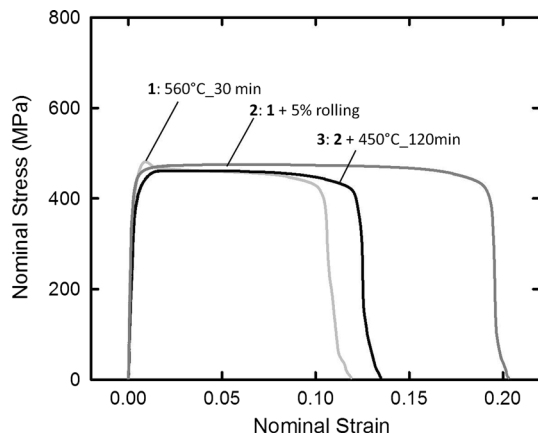


Fig. 7 Nominal stress–strain curves of the IF steel specimens. *Curve 1*: processed by 5 ARB cycles and annealed at 560 °C for 30 min. *Curve 2*: same material as 1, plus 5 % temper rolling at room temperature. *Curve 3*: same material as 2, plus low temperature annealing at 450 °C for 120 min

[5]. The stress–strain curve of the low temperature (450 °C) annealed specimen is shown as curve 3 in Fig. 7, which exhibits an obvious decrease in the uniform elongation (1.8 %) compared with curve 2. Although the specimen does not exhibit a sharp yield point, a yield plateau could be still found on the stress–strain curve, and thus it is considered that the specimen behaves a kind of discontinuous yielding behavior. A slight decrease in strength is found in this specimen compared with the temper-rolled specimen, which is likely to be due to the slight grain size coarsening by the low temperature annealing. Although further TEM observation is necessary to clarify the change in the microstructure, especially the dislocation structure after temper rolling and low temperature annealing, it can be realized from the present study that the uniform elongation of the fine-grained specimen is relatively high, when it exhibits continuous yielding or low, when it exhibits discontinuous yielding. The authors believe that the same explanation can be applied to the “hardening by annealing and softening by deformation” reported for the as-ARB processed materials. The as-ARB processed material is likely to have a medium mobile dislocation density which is introduced by the ARB process. Therefore, when the mobile dislocation density is increased by additional deformation, it exhibits a more continuous yielding behavior with a decreased strength and enhancement in the uniform elongation (*softening by deformation*). When the mobile dislocation density is decreased by low temperature annealing, the material exhibits a more discontinuous yielding behavior with an increased strength and reduction in the uniform elongation (*hardening by annealing*).

Conclusion

In the present study, IF steel specimens with different grain sizes ranging from 12 to 0.45 μm were fabricated by ARB process and subsequent annealing. Tensile tests at room temperature revealed a transition from continuous yielding to discontinuous yielding behaviors with decreasing the mean grain size down to an ultrafine range smaller than 1 μm . Two distinct Hall–Petch slopes were found, associated with the coarse grain size specimen exhibiting continuous yielding and the fine grain-sized specimen exhibiting discontinuous yielding. The dramatic drop in the uniform elongation was found to occur, when the grain size became below 1.5 μm . This dramatic drop was attributed to the enhanced early plastic instability associated with the occurrence of discontinuous yielding behavior in the fine-grained specimens, which could be explained by Hall–Petch analysis for the yield and flow stresses. By applying temper cold rolling or a low temperature annealing, the yielding behavior was changed between the two types, i.e., continuous type and discontinuous type, and the uniform elongation of the specimen also changed depending on different yielding behaviors. Since it has been found that discontinuous yielding is a unique mechanical behavior of various kinds of materials with fine grain sizes, it can be concluded that the yielding behavior has a significant importance on the ductility of nanostructured materials.

Acknowledgements This study was financially supported by the Grant-in-Aid for Scientific Research on Innovative Area, “Bulk Nanostructured Metals” (area No.2201), the Grant-in-Aid for Scientific Research (A) (No.24246114), and the Elements Strategy Initiative for Structural Materials (ESISM), all through the Ministry of Education, Culture, Sports, Science and Technology (MEXT), Japan (contact No. 22102002), and the supports are gratefully appreciated.

References

- Hall EO (1951) The deformation and ageing of mild steel. Proc Phys Soc B 64:747–753
- Petch NJ (1953) The cleavage strength of polycrystals. J Iron Steel Inst 174:25–28
- Tsuji N, Ito Y, Saito Y, Minamino Y (2002) Strength and ductility of ultrafine grained aluminum and iron produced by ARB and annealing. Scr Mater 47:893–899
- Huang X, Hansen N, Tsuji N (2006) Hardening by annealing and softening by deformation in nanostructured metals. Science 312:249–251
- Huang X, Kamikawa N, Hansen N (2010) Strengthening mechanisms and optimization of structure and properties in a nanostructured IF steel. J Mater Sci 45:4761–4769
- Kidmose J, Lu L, Winther G, Hansen N, Huang X (2012) Strain distribution during tensile deformation of nanostructured aluminum samples. J Mater Sci 47:7901–7907
- An H, Wu S, Zhang Z, Figueiredo RB, Gao N, Langdon TG (2012) Enhanced strength–ductility synergy in nanostructured Cu and Cu–Al alloys processed by high-pressure torsion and subsequent annealing. Scr Mater 66:227–230

8. Yu CY, Kao PW, Chang CP (2005) Transition of tensile deformation behaviors in ultrafine-grained aluminum. *Acta Mater* 53:4019–4028
9. Li Z, Fu L, Fu B, Shan A (2013) Yield point elongation in fine-grained titanium. *Mater Lett* 96:1–4
10. Kamikawa N, PhD thesis, 2005, Osaka University
11. Gao S, Chen M, Chen S, Kamikawa N, Shibata A, Tsuji N (2014) Yielding behavior and its effect on uniform elongation of fine grained IF steel. *Mater Trans* 55:73–77
12. Cottrell A, Bilby B (1949) Dislocation theory of yielding and strain ageing of iron. *Proc Phys Soc A* 49:49–62
13. Hahn GT (1962) A model for yielding with special reference to the yield-point phenomena of iron and related bcc metals. *Acta Metall* 10:727–738
14. Sabirov I, Estrin Y, Barnett MR, Timokhina I, Hodgson PD (2008) Tensile deformation of an ultrafine-grained aluminium alloy: micro shear banding and grain boundary sliding. *Acta Mater* 56:2223–2230
15. Saha R, Ueji R, Tsuji N (2013) Fully recrystallized nanostructure fabricated without severe plastic deformation in high-Mn austenitic steel. *Scr Mater* 68:813–816
16. Armstrong RW, Codd I, Douthwaite RM, Petch NJ (1962) The plastic deformation of polycrystalline aggregates. *Philos Mag* 7:45–57
17. Hall EO (1970) *Yield Point Phenomena in Metals and Alloys*. Springer, New York, pp 1–64